Role of $P_{13}(1720)$ in $K\Sigma$ photoproduction

T. Mart
Jurusan Fisika, FMIPA, Universitas Indonesia, Depok 16424, Indonesia
(Received 25 January 2000; published 26 July 2000)

Using an isobar model and the new SAPHIR data we show that a better explanation of $K^0\Sigma^+$ photoproduction can be achieved by including the $P_{13}(1720)$ resonance. We find that the inclusion of this state does not influence the $K^+\Sigma^0$ channel appreciably, in contrast to the other three $K\Sigma$ channels, where the prominent effect is found in the $K^0\Sigma^+$ channel. The extracted fractional decay width is consistent with the prediction of the quark model, whose magnitude is almost one order smaller than the value given by the Particle Data Group.

PACS number(s): 14.20.Gk, 25.20.Lj, 13.60.Le, 13.30.Eg

For more than 30 years kaon photoproduction on the nucleon has played a special role in the realm of strangeness physics. A simultaneous study of the kaon-hyperon-nucleon coupling constants, isospin symmetry, hadronic form factors, baryon and meson resonances, and the contribution of kaon-hyperon final states to the magnetic moment of the nucleon, is made possible only by means of this elementary process. In the hypernuclear sector, investigations of the electromagnetic production of hypernuclei would be unthinkable without a good understanding of the elementary process. In addition, the associated production on a deuteron can be used to study the hyperon-nucleon interaction in the final state, while the quasifree kaon photoproduction on nuclei serves as an important tool for investigating the kaon-nucleus and hyperon-nucleus optical potentials. These processes cannot be properly understood without an elementary operator that describes the production mechanism on the nuclear constituents. Along with the operation of the new generation of continuous electron-beam accelerators, such as CEBAF (now JLab), ELSA, and ESRF, as well as the new and more precise detectors, this fact has greatly motivated considerable efforts to advance our knowledge of the process.

It has been well known that there are six possible isospin channels in kaon photoproduction, i.e.,

$$p(\gamma,K^+)\Lambda, \quad p(\gamma,K^+)\Sigma^0, \quad p(\gamma,K^0)\Sigma^+ \quad \text{on the proton,}$$

$$n(\gamma,K^0)\Lambda, \quad n(\gamma,K^+)\Sigma^-, \quad n(\gamma,K^0)\Sigma^0 \quad \text{on the neutron.}$$

However, only the first two reactions were extensively studied during the past years [1–5] since most experimental data exist only for those two channels. There were only few investigations devoted to the third process, since there were only two data points (in the total cross section) for this channel. However, a previous study [6] has shown that this channel could provide a strong constraint to the models that try to explain kaon photoproduction on the proton. Due to the lack of a neutron target, there are no data available in the neutron channels up to now, although Ref. [6] has also marked that these channels are sensitive to the resonance configuration in the models and, as a consequence, provide additional constraints to the models.

Recently, we have developed a new elementary operator for kaon photoproduction on the nucleon [7]. The background part of the operator consists of the standard Born terms along with the $K^*(892)$ and $K_1(1270)$ vector meson poles in the t channel. The low-energy resonance part of the $K\Lambda$ operator includes three states that have been found to have significant decay widths into the $K^+\Lambda$ channel, the $S_{11}(1650)$, $P_{11}(1710)$, and $P_{13}(1720)$ resonances. In order to take into account the fact that baryons and mesons are not pointlike, we include hadronic form factors by employing the gauge method of Haberzettl [8]. The fit to the data was significantly improved by allowing for separate cutoffs for the background and resonant sector. An excellent agreement between experimental data and model prediction has been achieved, where it is then found that a new, missing, $D_{13}(1895)$ nucleon resonance appears naturally in order to explain the apparent structure in the total cross section of the SAPHIR data [9].

However, the situation is different in $K\Sigma$ channels, where experimental data cannot be obtained as precisely as those in

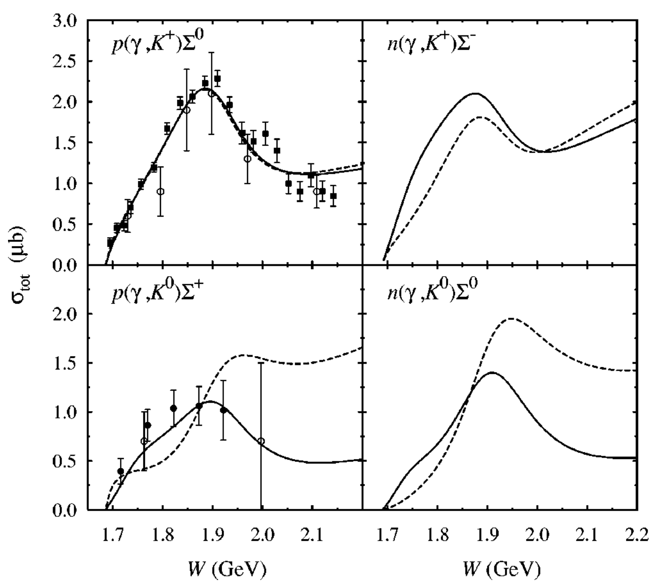

FIG. 1. Total cross sections for $K\Sigma$ photoproduction. Dashed lines show the fit to $K\Sigma$ data without the $P_{13}(1720)$ resonance, solid lines are obtained by including this resonance in the model. Experimental data from SAPHIR are shown by the solid squares [10] and solid circles [11]. Old data are displayed by the open circles [12].

0556-2813/2000/62(3)/038201(4)/$15.00

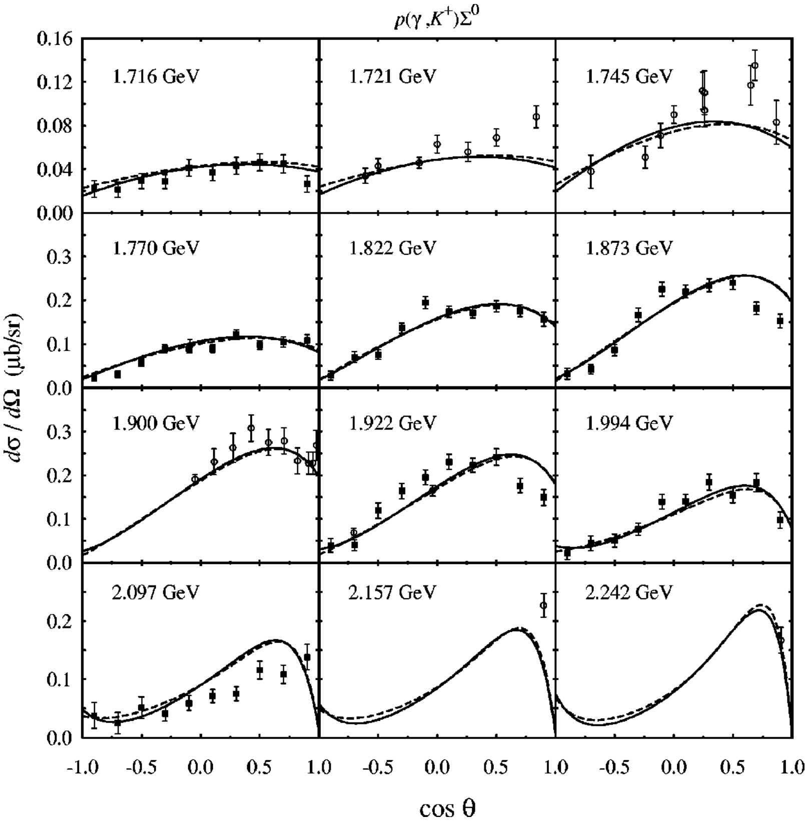

FIG. 2. Same as in Fig. 1 for the $p(\gamma,K^+)\Sigma^0$ differential cross section. The total c.m. energy W is shown in every panel.

the $K\Lambda$ channel. This is chiefly due to the intrinsic properties of the Σ hyperons, which are relatively more difficult to observe. Moreover, the isospin conservation allows Δ resonances to contribute in $K\Sigma$ processes. Thus, in principle, the elementary operator for $K\Sigma$ photoproduction should be more complicated than that of $K\Lambda$. This was, however, not completely true in our previous model [7], where the same background terms, as in the $K\Lambda$ case, combined with two low-lying nucleon resonances, the $S_{11}(1650)$ and $P_{11}(1710)$, along with two more spin 1/2 Δ, the $S_{31}(1900)$ and $P_{31}(1910)$, were quite sufficient to describe the available data, including the preliminary version of $K^0\Sigma^+$ SAPHIR data.

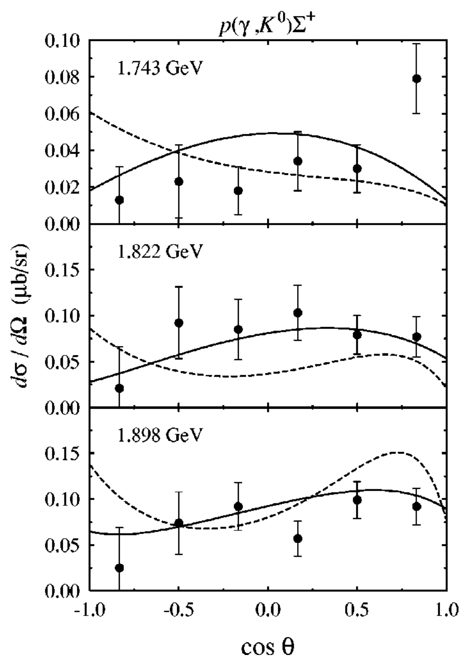

FIG. 3. Same as in Fig. 1 for the $p(\gamma,K^0)\Sigma^+$ differential cross section. The total c.m. energy W is shown in every panel.

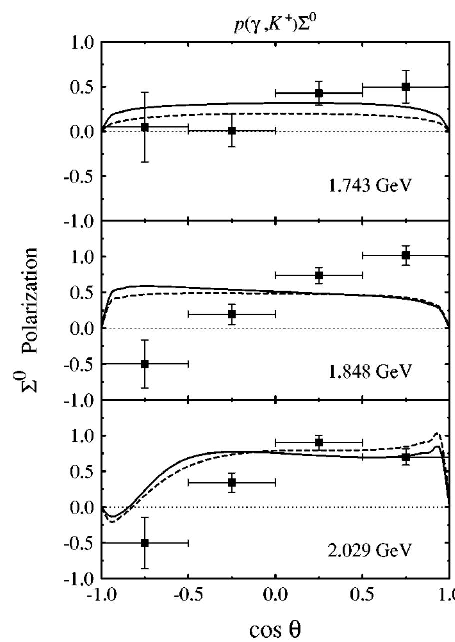

FIG. 4. Same as in Fig. 1 for the Σ^0 polarization. The total c.m. energy W is shown in every panel.

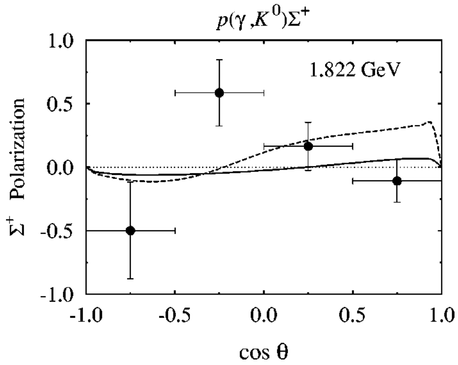

FIG. 5. Same as in Fig. 1 for the Σ^+ polarization. The total c.m. energy W is shown in the figure.

Very recently, the final version of $K^0\Sigma^+$ SAPHIR data has been published in Ref. [11]. Our previous model immediately faces an obvious problem; the present data have an average magnitude of about 50% smaller than the preliminary ones. To overcome this, we try to refit our previous model to all existing $K\Sigma$ data, including the new version of $K^0\Sigma^+$ data. Unfortunately, as shown in Fig. 1, the problem persists in the $K^0\Sigma^+$ total cross section, i.e., the model cannot reproduce the shape of the total cross section.

Based on the same reasoning as in the $K\Lambda$ case [9], we include the $P_{13}(1720)$ intermediate state in our $K\Sigma$ model. This choice seems to be somewhat trivial, but previous studies have indicated the importance of this resonance in $K\Sigma$ channels. For instance, Ref. [4] found that the $P_{13}(1720)$ contributes less than 10% to the $K^+\Sigma^0$ channel, but dominates the $K^0\Sigma^+$ process up to more than 40%, although in the latter the fit was performed with only two (old) data points in the total cross section.

Within this new resonance configuration the χ^2/N reduces from about 2.5 to 2.3 and the result is shown in Fig. 1 by the solid lines, where one may argue that, apart from the rapid convergence of the $K^0\Sigma^+$ total cross section, the remarkable agreement with the data is not so surprising since we have added two more free parameters in the fit. Nevertheless, the important point to note here is the different effects of the $P_{13}(1720)$ resonance on those two proton channels. As shown in Fig. 1 the effect is small in the $K^+\Sigma^0$ channel, but quite substantial in the $K^0\Sigma^+$ channel. Obviously, this finding explains why we did not observe the role of the $P_{13}(1720)$ resonance in $K\Sigma$ channels in our previous model. Furthermore, the two neutron channels shown in Fig. 1 reveal that both channels are the good candidates for further investigating this resonance.

On the other hand, this result might also raise a question, since the inclusion of the $P_{13}(1720)$ resonance seems to affect the cross section in the whole energy regions. This happens because the $P_{13}(1720)$ mass is very close to the production threshold, thus almost overlapping with those of the other two nucleon resonances. After including this resonance, the fit readjusts the coupling constants to the values which decrease contributions from the t-channel poles at higher energies. As shown in the previous study [7], the $K^*(892)$ and $K_1(1270)$ vector meson are responsible for the divergence behavior of cross sections at higher energies.

Compared with the previous work on isobar model [4], our model exhibits a much better agreement with the $K^0\Sigma^+$ total cross section data. Their model suffers mainly from the divergence of the cross section since no hadronic form factors are considered. There has been an effort to remedy this undesirable situation by taking into account the off-shell effects of certain resonances [13], which is, however, beyond the scope of the present work. Compared with the results from the recent chiral coupled-channels approach [14], we observe that in both proton channels shown in Fig. 1 our model yields a better agreement with experimental data.

The same effects also appear in the differential cross sections as displayed in Figs. 2 and 3. One can clearly see here, that the angular distribution is almost unaffected by the inclusion of the $P_{13}(1720)$ resonance in the first case, whereas in the second case the differential cross sections are significantly improved after we include this state. Note that without this intermediate state the model yields a wrong "backward-peaking" behavior, in contrast to the structure exhibited by the new SAPHIR data.

The recoil polarizations for the two channels are shown in Figs. 4 and 5. Here we obtain a fair agreement with the data. Since the polarization observables stem purely from resonance contributions, this perhaps indicates that the resonance configuration in our $K\Sigma$ model is not yet final. However, at this stage it is worth to note that the data shown here have been averaged in relatively large energy bins, especially in the latter, where the four data points were binned in the energy range between threshold and $W = 1.898$ GeV. Therefore, in our opinion, more statistics in the data should be obtained first before any further conclusion could be drawn. To our knowledge, up to now there has been no model that successfully reproduces these polarization observables. The recent chiral coupled-channels approach [14] works only for the data shown in the upper panel of Fig. 4, but it fails to reproduce the oscillation in the Σ^+ polarization.

TABLE I. The fractional decay width of $P_{13}(1720)$ from the quark model [15], PDG listing (as given also in Ref. [15]), and the present work. In view of the current error bar in our database, we omit all error bars in this table. Therefore, in the last column, only the order of magnitude is relevant to our present discussion.

Source	M_{N*} (MeV)	Γ_{N*} (MeV)	$\sqrt{\Gamma_{N*N\gamma}}$ (MeV$^{1/2}$)	$\sqrt{\Gamma_{N*K\Sigma}}$ (MeV$^{1/2}$)	$\sqrt{\Gamma_{N*N\gamma}\Gamma_{N*K\Sigma}}/\Gamma_{N*}$
Quark model	1795	150	0.085	0.3	0.17×10^{-3}
PDG	1720	150	0.091	2.2	1.33×10^{-3}
This work	1720	150			0.20×10^{-3}

Although the calculation given here is less accurate than our previous study of the $K^+\Lambda$ channel [9], it is still appealing to compare the extracted coupling constants with prediction of the constituent quark model [15] and those given by the Particle Data Group (PDG) listings. As shown in Table I, surprisingly, our naive calculation confirms the result from quark model, which therefore builds a consistency with the previous investigation of the $K\Lambda$ channel [9]. Table I reveals that the value given by the PDG turns out to be almost one order of magnitude larger than our result.

In conclusion, we have investigated the role of the $P_{13}(1720)$ resonance in photoproduction of $K\Sigma$ in the framework of an isobar model. Our findings corroborate the result from previous work that this state is required in order to explain the $K^0\Sigma^+$ data. The extracted coupling constants are in good agreement with the prediction from the quark model; a result which is also found in the $K\Lambda$ case. To further elucidate the role of this state, more accurate $K^0\Sigma^+$ data are advocated, especially in the polarization observables. Measurements of $K\Sigma$ photoproduction on the neutron will also provide more information to shed additional light on this problem. Finally, we should mention that due to the nature of the findings in this exploratory study, a rigorous, unitary, and more consistent investigation performed in the framework of multichannels analyses is strongly urged.

This work was supported in part by a University Research for Graduate Education (URGE) grant.

[1] R. A. Adelseck, C. Bennhold, and L. E. Wright, Phys. Rev. C **32**, 1681 (1985).

[2] R. A. Adelseck and B. Saghai, Phys. Rev. C **42**, 108 (1990).

[3] R. A. Williams, C.-R. Ji, and S. R. Cotanch, Phys. Rev. C **46**, 1617 (1992).

[4] J. C. David, C. Fayard, G. H. Lamot, and B. Saghai, Phys. Rev. C **53**, 2613 (1996).

[5] B. S. Han, M. K. Cheoun, K. S. Kim, and I.-T. Cheon, nucl-th/9912011.

[6] T. Mart, C. Bennhold, and C. E. Hyde-Wright, Phys. Rev. C **51**, R1074 (1995).

[7] F. X. Lee, T. Mart, C. Bennhold, and L. E. Wright, nucl-th/9907119.

[8] H. Haberzettl, C. Bennhold, T. Mart, and T. Feuster, Phys. Rev. C **58**, R40 (1998).

[9] T. Mart and C. Bennhold, Phys. Rev. C **61**, 012201(R) (2000).

[10] M. Q. Tran *et al.*, Phys. Lett. B **445**, 20 (1998).

[11] S. Goers *et al.*, Phys. Lett. B **464**, 331 (1999).

[12] ABBHHM Collaboration, Phys. Rev. **188**, 2060 (1969).

[13] T. Mizutani, C. Fayard, G. H. Lamot, and B. Saghai, Phys. Rev. C **58**, 75 (1998).

[14] J. C. Ramon, N. Kaiser, S. Wetzel, and W. Weise, Nucl. Phys. **A672**, 249 (2000).

[15] S. Capstick, Phys. Rev. D **46**, 2864 (1992); S. Capstick and W. Roberts, *ibid.* **58**, 074011 (1998).